

# Development of potent monoclonal antibody auristatin conjugates for cancer therapy

Svetlana O Doronina, Brian E Toki, Michael Y Torgov, Brian A Mendelsohn, Charles G Cervený, Dana F Chace, Ron L DeBlanc, R Patrick Gearing, Tim D Bovee, Clay B Siegall, Joseph A Francisco, Alan F Wahl, Damon L Meyer & Peter D Senter

We describe the *in vitro* and *in vivo* properties of monoclonal antibody (mAb)-drug conjugates consisting of the potent synthetic dolastatin 10 analogs auristatin E (AE) and monomethylauristatin E (MMAE), linked to the chimeric mAbs cBR96 (specific to Lewis Y on carcinomas) and cAC10 (specific to CD30 on hematological malignancies). The linkers used for conjugate formation included an acid-labile hydrazone and protease-sensitive dipeptides, leading to uniformly substituted conjugates that efficiently released active drug in the lysosomes of antigen-positive (Ag<sup>+</sup>) tumor cells. The peptide-linked mAb-valine-citrulline-MMAE and mAb-phenylalanine-lysine-MMAE conjugates were much more stable in buffers and plasma than the conjugates of mAb and the hydrazone of 5-benzoylvaleric acid-AE ester (AEVB). As a result, the mAb-Val-Cit-MMAE conjugates exhibited greater *in vitro* specificity and lower *in vivo* toxicity than corresponding hydrazone conjugates. *In vivo* studies demonstrated that the peptide-linked conjugates induced regressions and cures of established tumor xenografts with therapeutic indices as high as 60-fold. These conjugates illustrate the importance of linker technology, drug potency and conjugation methodology in developing safe and efficacious mAb-drug conjugates for cancer therapy.

mAbs and mAb-based reagents have shown considerable effectiveness in the clinical treatment of cancer<sup>1,2</sup>. In light of the efficacy of such agents as Rituxan (rituximab) in treatment of non-Hodgkin lymphoma<sup>3</sup>, Panorex (edrecolomab) in colorectal carcinoma<sup>4</sup> and Herceptin (trastuzumab) in metastatic breast cancer<sup>5</sup>, there has been a resurgence of interest in using mAbs as vehicles for the delivery of cytotoxic agents to tumor cells. The objective of this approach is to enhance drug efficacy through targeted delivery, while sparing nontarget tissues from chemotherapeutic damage<sup>6</sup>.

A major advance in mAb-mediated drug delivery was made with the development of Mylotarg, the only conjugate thus far clinically approved<sup>7</sup>. Mylotarg is composed of an mAb specific to CD33, linked to the highly potent DNA-alkylating agent calicheamicin through an acid-labile hydrazone bond<sup>8,9</sup>. In clinical studies Mylotarg has shown efficacy against acute myeloid leukemia, even though both the drug and the linker used to attach it to the mAb are relatively unstable under physiological conditions, and the preparation is highly heterogeneous, with only ~50% of the mAb actually existing in the conjugated form<sup>7</sup>. Other conjugates containing doxorubicin<sup>10,11</sup>, a maytansinoid<sup>12</sup>, analogs of CC-1065 (ref. 13) and a potent taxoid<sup>14</sup> have been reported and are at various stages of pre-clinical and early clinical investigation. Although these conjugates have elicited pronounced antitumor activities in xenograft models, their efficacy is hindered by low drug potency<sup>10,11</sup>, linker instability<sup>10-14</sup> and compositional heterogeneity<sup>12-14</sup>. As a result, activity in preclinical xenograft models has required either very high doses<sup>10</sup> or doses very close to those that are maximally tolerated<sup>12,13</sup>. For the clinical treatment of solid tumors in which intratumoral conjugate

uptake is slow and limited<sup>15</sup>, such conjugates would be expected to be suboptimal.

Given the potential impact of mAb-targeted drug delivery on cancer medicine, there is an urgent need to address these issues. Toward this end, we set out to develop a new class of immunoconjugates consisting of potent, synthetic cytotoxic agents linked in a highly stable fashion to internalizing mAbs. The peptide-based linkers were designed to facilitate rapid and efficient drug cleavage inside the target cell population<sup>16-20</sup>. Here, we report the use of cathepsin B-cleavable peptide linkers to attach a potent and very stable antimitotic agent, MMAE, to mAbs. The stability characteristics, *in vitro* properties and *in vivo* activities of these conjugates are compared to AE conjugates linked through conventional and less stable acid-labile hydrazones. The highly optimized peptide-linked conjugates effect immunologically specific cell kill, lead to regressions and cures of established tumor xenografts at well-tolerated doses and display therapeutic indices as high as 60-fold, a significant advance over other mAb-drug conjugates. The results underscore the importance of drug stability and potency, conditional linker stability and conjugate homogeneity in developing effective conjugates for cancer therapy.

## RESULTS

### Preparation of mAb-auristatin conjugates

AE and MMAE (Fig. 1) are structurally related to dolastatin 10, a pentapeptide natural product that has been the subject of several human clinical trials for cancer therapy<sup>21-23</sup>. Molecules in this family exert potent antitumor activities by inhibiting tubulin polymerization, and may also cause intratumoral vascular damage<sup>24</sup>. The cytotoxic effects

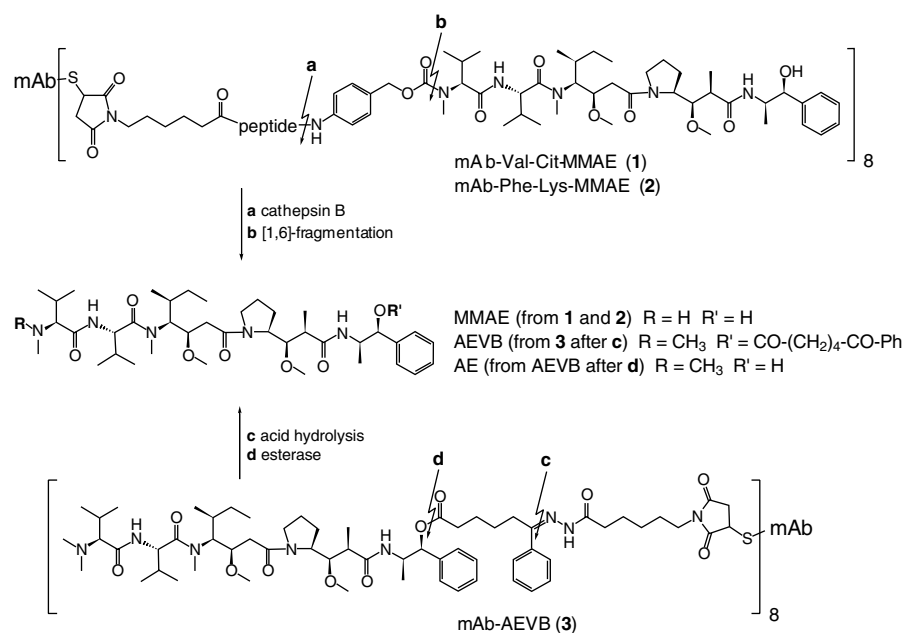


**Figure 1** Structures of drugs and mAb-drug conjugates. Drug is released from the peptide conjugates 1 and 2 through enzymatic hydrolysis (step a) and spontaneous fragmentation (step b) of the *p*-aminobenzylcarbamate intermediate. Drug is released from mAb-AEVB conjugates (3) through hydrazone hydrolysis (step c) and hydrolysis of the ester (step d).

of AE were evaluated on a diverse panel of 39 human tumor cell lines including hematological malignancies, melanoma, and carcinomas of the lung, stomach, prostate, ovaries, pancreas, breast, colon and kidneys, and were compared to the activities of another antimitotic agent, vinblastine, as well as to doxorubicin. The results (data not shown) indicated that none of the cell lines was resistant to AE, and that the drug (average half-maximal inhibitory concentration (IC<sub>50</sub>) 3.2 ± 0.51 nM, 1 h exposure) was 52- and 197-fold more potent than vinblastine (average IC<sub>50</sub> 166 nM) and doxorubicin (average IC<sub>50</sub> 631 nM), respectively. On a panel of seven human lymphoma cell lines, the average IC<sub>50</sub> value of AE was 1.4 nM; this is comparable to *N*-acetyl- $\gamma$ -calicheamicin, the cytotoxic component of Mylotarg, which has an IC<sub>50</sub> value of ~4.3 nM on leukemia and lymphoma cell lines<sup>8,9</sup>.

The syntheses of AE and MMAE proceeded through highly convergent routes<sup>25</sup>, allowing for routine preparation of multigram quantities. Because AE and MMAE are totally synthetic, it was possible to incorporate functional groups for mAb attachment through a variety of linkage strategies. We focused on acid-labile and proteolytically cleavable linkers, because mAbs that are internalized through receptor-mediated endocytosis commonly traffic through lysosomes that are both acidic and rich in highly active proteases<sup>6</sup>. Acid-labile linkers, containing hydrazone functionalities as the cleavable moiety, were formed at the C terminus of AE by condensing maleimidocaproyl hydrazide with a panel of AE ketoesters. AEVB (Fig. 1) was selected for additional studies because it was relatively stable at pH 7.2 (*t*<sub>1/2</sub> > 60 h) but was labile at pH 5.0 (*t*<sub>1/2</sub> 3 h). Protease-cleavable dipeptide linkers were attached to the N-terminal position of MMAE through a self-immolative *p*-aminobenzylcarbamate spacer<sup>16,17,26</sup>. Consistent with previous findings with peptide derivatives of doxorubicin<sup>16,17</sup>, Phe-Lys-MMAE and Val-Cit-MMAE were quite stable under physiological conditions but underwent rapid hydrolysis, leading to the release of MMAE in the presence of lysosomal extracts and purified human cathepsin B, a tumor-associated lysosomal enzyme<sup>6,27</sup>.

Conjugates of MMAE and AEVB were formed using the chimeric mAbs cBR96 (ref. 10) and cAC10 (ref. 28), recognizing the Lewis Y antigen on carcinomas and the CD30 antigen on hematological malignancies, respectively. The mAbs were reduced and then alkylated with the maleimido-containing MMAE and AEVB drug derivatives, forming nonaggregated conjugates with about eight drugs attached per mAb (Fig. 1). This reductive conjugation method preserves mAb affinity, is applicable to many IgGs, leads to a high degree of conjugate uniformity and proceeds with yields in the range of 80% based on the mAb component. Importantly, size-exclusion high-performance liquid chromatography (HPLC) showed that the conjugates thus produced were not aggregated (Fig. 2a), and fluorescence-activated cell sorting (FACS) analysis (Fig. 2b) indicated that the binding characteristics were preserved.

#### Drug and conjugate stability

AE and MMAE are highly stable molecules. There were no signs of compound degradation after 16 d in buffered saline at 37 °C. Furthermore, there was no evidence for drug

metabolism or decomposition in the presence of human liver lysosomal extracts, or with lysosomal proteases such as cathepsin B.

Incubation of cBR96-Val-Cit-MMAE and cBR96-Phe-Lys-MMAE with purified human cathepsin B resulted in the release of MMAE with specific activities of 360 and 670 nmol/min/mg, respectively (Fig. 2c). The aminobenzylcarbamate intermediate (Fig. 1) was undetectable by HPLC analysis, because of the very rapid nature of the [1,6]-fragmentation reaction<sup>26</sup>. SDS-PAGE analysis for both conjugates demonstrated that cathepsin B treatment induced a mobility shift for both the heavy and light chains (Fig. 2d), in agreement with the HPLC-derived kinetic data for drug release. These data suggest that cathepsin B effects efficient drug release without concomitant mAb degradation. Related liquid chromatography–tandem mass spectrometry (LC-MS/MS) studies with the acid-labile cBR96-AEVB conjugate established that free AEVB was released nonenzymatically at pH 5 (*t*<sub>1/2</sub> 4.4 h) more rapidly than at pH 7.2 (*t*<sub>1/2</sub> 183 h). Taken together, these results show that both the protease and acid-labile linker strategies lead to well-defined conjugates in which parent drug release proceeds under conditions present within the lysosomes of target cells.

The stability characteristics of the cBR96 conjugates in human and mouse plasma at 37 °C are shown in Figure 3. In human plasma, AEVB was the predominant species formed initially, and AE accumulated over time (Fig. 3a). This is consistent with the drug release sequence shown in Figure 1, with hydrazone hydrolysis taking place first and ester hydrolysis second. In mouse plasma (Fig. 3b), the total amount of drug released at each time point was similar to that in human plasma, but the predominant species was AE. Because mouse plasma has much higher levels of esterase activity than human plasma<sup>29</sup>, the released AEVB was most likely rapidly hydrolyzed and never accumulated. Drug release in both plasma samples was rapid, with half-lives of 2.6 and 2.1 d in human and mouse plasma, respectively.

The dipeptide-linked conjugates were much more stable in plasma than the hydrazone conjugate, and MMAE was the only detectable

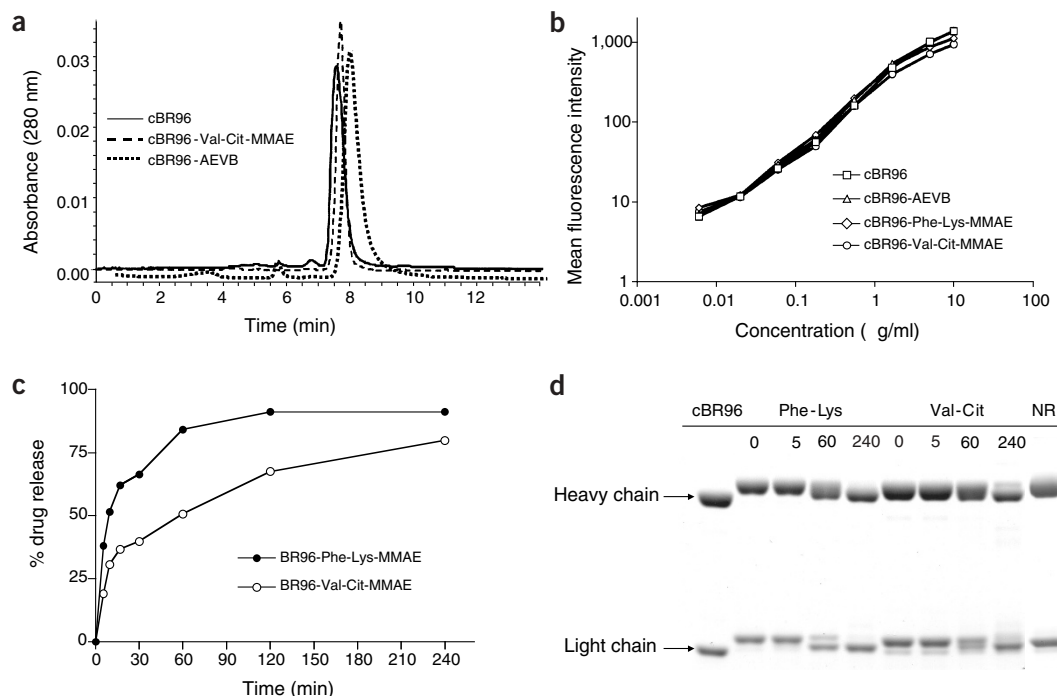


**Figure 2** Conjugate characteristics. (a) Size-exclusion HPLC analysis of cBR96 and cBR96 conjugates with approximately eight drug-mAb combinations. (b) Binding of cBR96 and cBR96 conjugates to Lewis Y<sup>+</sup> RCA colorectal carcinoma cell, as determined by FACS analysis. (c) Hydrolysis of cBR96-Phe-Lys-MMAE and cBR96-Val-Cit-MMAE (eight drug-mAb combinations) with human cathepsin B (4 μg/ml, pH 5, 37 °C). Drug release was monitored and quantified by RP-HPLC. (d) SDS-PAGE (12%) analysis of denatured cBR96 (lane 1), and the cBR96-Phe-Lys-MMAE (lanes 2–5) and cBR96-Val-Cit-MMAE (lanes 6–9) conjugates from human cathepsin B treatment. The cBR96-Val-Cit-MMAE conjugate under nonreducing (NR) conditions is shown in lane 10. Hydrolysis times are indicated in minutes. Cathepsin B cleaves the bond between the *p*-aminobenzyl group and the peptide (Fig. 1), leading to drug release and progressively lower apparent masses for the heavy and light chains.

drug released. Drug release was faster in mouse plasma than in human plasma, and in both plasma types the Val-Cit peptide (Fig. 3c) was more stable than Phe-Lys (Fig. 3d). The projected half-lives for the Val-Cit-linked drug were 30 and 230 d in mouse and human plasma, respectively. The corresponding projected half-lives for the Phe-Lys-linked drug were 12.5 and 80 d. Thus, the peptide linkers impart much greater plasma stability than the hydrazone linker.

**In vitro cytotoxicity**

The cytotoxic effects of the conjugates on H3396 cells (cBR96 Ag<sup>+</sup>, cAC10 Ag<sup>-</sup>) were determined using both pulsed (2 h) and long-term (96 h) drug exposure assays. Under both exposure conditions, high degrees of immunological specificity were obtained with the Val-Cit conjugates, because cAC10-Val-Cit-MMAE had no activity whereas cBR96-Val-Cit-MMAE was highly active at <1/100th of the concentration required for antigen saturation (Fig. 4a). The lack of activity for cAC10-Val-Cit-MMAE even after 96 h of continuous exposure further illustrates the stability of the peptide-linked conjugates. In contrast, the hydrazone conjugates were marginally specific in the 2-h pulse assay, and were completely nonspecific after continuous exposure (Fig. 4b), consistent with hydrazone hydrolysis in the course of the assay. Similar experiments were undertaken with Karpas 299 anaplastic large cell lymphoma (ALCL) cells that express the CD30 but not the Lewis Y antigens (Fig. 4c). In the 96-h continuous exposure assay, the effects of the Val-Cit conjugates were immunologically specific, whereas there was only a fivefold difference in potency between the binding and non-binding AEVB conjugates. Further insight into the cytotoxic activities was obtained using a clonogenic assay on RCA colorectal carcinoma

cells (cBR96 Ag<sup>+</sup>, cAC10 Ag<sup>-</sup>) that were treated with the mAb-Val-Cit-MMAE conjugates for 96 h (Fig. 4d). Under these conditions, there was as much as a 10<sup>4</sup>-fold reduction in cell viability in cBR96-Val-Cit-MMAE-treated cells, a result that was not reflected in the less sensitive Alamar Blue assay. Table 1 illustrates the activities of the mAb-Val-Cit-MMAE conjugates on a panel of cell lines. In all cases, the conjugates are potent, and the effects are due to specific drug delivery, because unconjugated, non-cross-linked mAbs have little to no cytotoxic activities<sup>10,28</sup>. In summary, both linker chemistries led to highly potent conjugates, with the peptide conjugates possessing greater immunological specificity probably because of their stability characteristics.

**In vivo studies**

The maximum tolerated doses (MTDs) of the mAb-Val-Cit-MMAE and mAb-AEVB conjugates were determined in tumor-free athymic and SCID mice after intravenous (i.v.) injection. It was possible to safely inject mAb-Val-Cit-MMAE conjugates at 30 mg mAb component/kg (contains 1.1 mg/kg MMAE component) without inducing weight loss or any overt signs of toxicity. Administration of 40 mg mAb component/kg resulted in substantial (>20%) weight loss and was not well tolerated. Therefore, the MTD of the mAb-Val-Cit-MMAE conjugates was 30 mg/kg. The mAb-AEVB conjugates were considerably more toxic, with MTDs of 15 mg mAb component/kg (contains 0.54 mg/kg AE drug component). The MTDs of single-dose injections of AE and MMAE were ~0.5 and 1.0 mg/kg, respectively.

*In vivo* therapy experiments were undertaken in athymic mice with subcutaneous L2987 human lung adenocarcinoma xenografts (cBR96 Ag<sup>+</sup>, cAC10 Ag<sup>-</sup>). Conjugates were administered at 3 mg mAb

mpg © 2003 Nature Publishing Group http://www.nature.com/naturebiotechnology

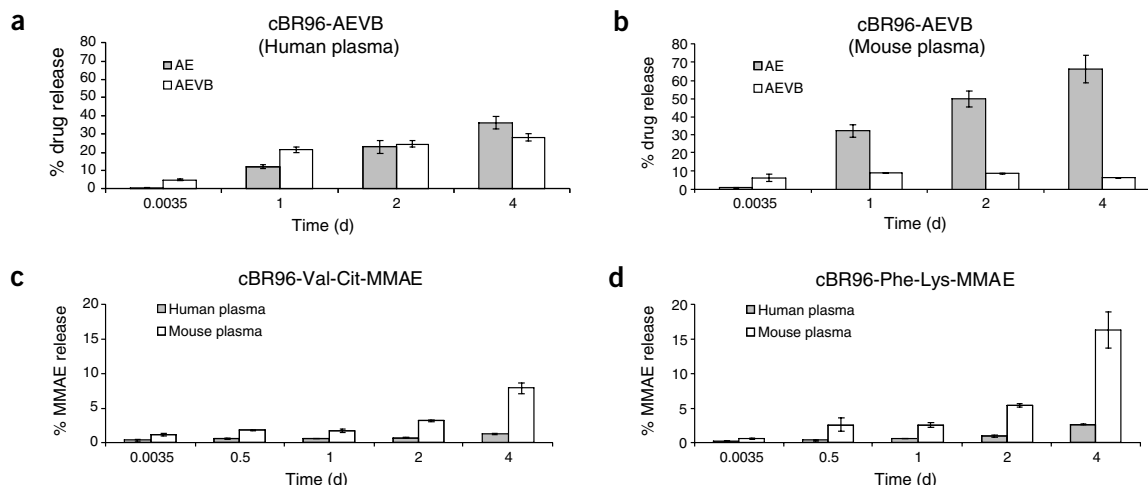


**Figure 3** Conjugate stability in human and mouse plasma. (a,b) cBR96-AEVB in (a) human and (b) mouse plasma was incubated at 37 °C, and at the times indicated, plasma proteins were precipitated with solvent and the total amount of AE and AEVB were quantified by LC-MS/MS. (c,d) Di-peptide-linked conjugates (c) cBR96-Val-Cit-MMAE and (d) cBR96-Phe-Lys-MMAE were similarly analyzed, but free MMAE was separated from plasma proteins by solid-phase extraction. In all cases, free drug was quantified by comparison to an authentic drug standard curve. Internal standards were included in all samples to determine extraction efficiencies.

component/kg/dose according to the schedule shown in Figure 5a, after the tumors had grown to ~100 mm<sup>3</sup>. All of the cBR96 conjugates were highly efficacious, leading to long-term regressions of established tumors at ~10% of the MTD, whereas the nonbinding control cAC10 conjugates had no effect on tumor growth. There were no apparent toxicities associated with conjugate treatment, and there was no statistical difference in activities between the various cBR96 conjugates shown in Figure 5a.

The results from the *in vivo* experiment, taken together with the stability and *in vitro* activities already described, prompted us to focus further attention on mAb-Val-Cit-MMAE conjugates. An experiment was undertaken in SCID mice with subcutaneous Karpas 299 ALCL tumors (cBR96 Ag<sup>-</sup>, cAC10Ag<sup>+</sup>), in which the cAC10-Val-Cit-MMAE was now the binding conjugate, whereas cBR96-Val-Cit-MMAE was the non-binding control. The therapeutic effects of cAC10-Val-Cit-MMAE were

pronounced (Fig. 5b). Cures of relatively large tumors (>200 mm<sup>3</sup>) were obtained at 1 mg mAb component/kg/injection (0.035 mg MMAE component/kg/injection), corresponding to 1/30th of the MTD. Equivalent doses of the nonbinding control conjugate, cBR96-Val-Cit-MMAE, were ineffective. Unconjugated MMAE, representing 10 times the amount of MMAE present within the conjugates, induced tumor regressions, but the effects were temporary. The cAC10 mAb had no antitumor activity in SCID mice with Karpas 299 tumor xenografts, nor did a combination of unconjugated cAC10 with the same amount of MMAE present in a 1 mg conjugate/kg/injection dose (Fig. 5c). Treatment with cAC10-Val-Cit-MMAE at 1 mg mAb component/kg/injection and at 0.5 mg/kg/injection resulted in 100% and 80% tumor cures, respectively (Fig. 5b,c). Thus, mAb-Val-Cit-MMAE conjugates lead to cures and regressions of established human ALCL tumor xenografts with immunological specificity at doses as low as 1/60th the MTD.

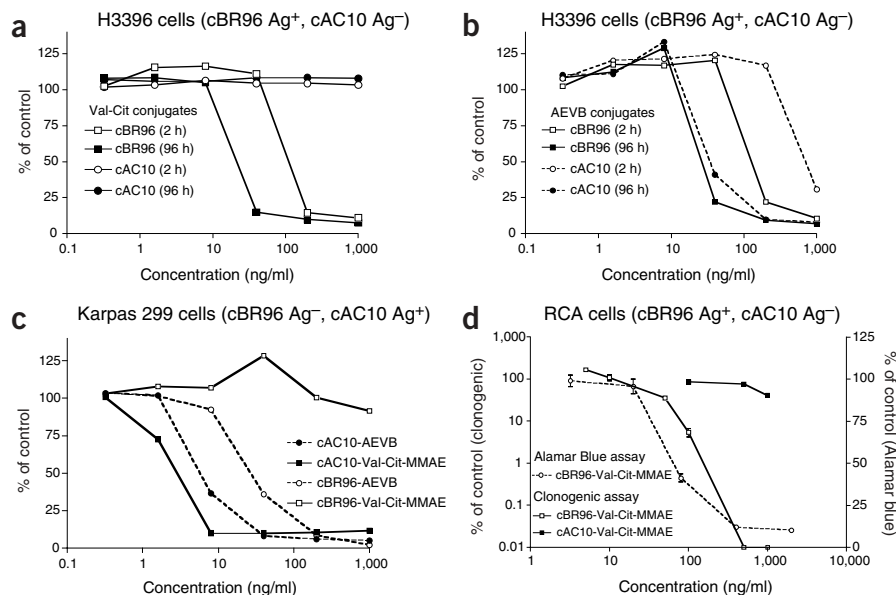


**Figure 4** *In vitro* cytotoxicity. (a–c) Alamar Blue conversion was used to measure the cytotoxic effects of the conjugates on cell lines. (a,b) Cytotoxic effects on H3396 human breast carcinoma cells (cBR96 Ag<sup>+</sup>, cAC10 Ag<sup>-</sup>). (c) Karpas 299 human ALCL cells (cAC10 Ag<sup>+</sup>, cBR96 Ag<sup>-</sup>). The cells were incubated with the conjugates continuously for 96 h, and the cytotoxic effects were determined by metabolism of Alamar Blue during the last 4 h of incubation. In some cases, as indicated in a and b, cells were pulsed with conjugate for 2 h and then washed; the cytotoxic effects were determined after 96 h. (d) The cytotoxic effects of the conjugates on RCA human colorectal carcinoma cells (cBR96 Ag<sup>+</sup>, cIgG Ag<sup>-</sup>) were determined using a clonogenic assay, and the results were compared to those obtained using Alamar Blue.

**Table 1** *In vitro* activities of mAb-Val-Cit-MMAE conjugates using Alamar Blue conversion as an indicator of cell viability

Cell line (type)	Antigen (expression) <sup>a</sup>	IC <sub>50</sub> (ng/ml)	Specificity ratio <sup>b</sup>
Karpas 299 (ALCL)	CD30 <sup>+</sup> (579)	4.5	>500
L540cy (Hodgkin's lymphoma)	CD30 <sup>+</sup> (495)	63	160
CESS (B-lymphoblastoid)	CD30 <sup>+</sup> (116)	6	>300
KM-H2 (Hodgkin's lymphoma)	CD30 <sup>+</sup> (102)	90	110
SKBR-3 (breast carcinoma)	LeY <sup>+</sup> (3500)	13	300
OVCAR-3 (ovarian carcinoma)	LeY <sup>+</sup> (2111)	10	53
MDA-MB-453 (breast carcinoma)	LeY <sup>+</sup> (922)	80	100
H3396 (breast carcinoma)	LeY <sup>+</sup> (755)	18	>50
RCA (colorectal carcinoma)	LeY <sup>+</sup> (664)	80	>120
MCF-7 (breast carcinoma)	LeY <sup>+</sup> (600)	80	125

<sup>a</sup>Antigen expression was determined by FACS analysis using cAC10 for CD30<sup>+</sup> cell lines and cBR96 for Lewis Y<sup>+</sup> (LeY<sup>+</sup>) cell lines. The numbers in parentheses are the mean channel fluorescence intensities. <sup>b</sup>The specificity ratio is the IC<sub>50</sub> value ratio of nonbinding conjugates to the binding control. In all cases, cAC10-Val-Cit-MMAE was used as a positive control for CD30<sup>+</sup> cell lines and as a negative control for LeY<sup>+</sup> cell lines, and cBR96-Val-Cit-MMAE was used as a positive control for LeY<sup>+</sup> cell lines, and as a negative control for CD30<sup>+</sup> cell lines.

**DISCUSSION**

The peptide-linked conjugates reported here are distinguished from conjugates described elsewhere in many ways: the drugs are potent, stable and synthetic; the linkers are highly stable in plasma, and the mAbs are site-specifically modified with a uniform number of drugs. These aspects are important in developing highly optimized conjugates for cancer therapy. For example, the cytotoxic entities, AE and MMAE, were prepared through convergent routes that allowed for the incorporation of almost any cleavable linker of interest. We focused on hydrazones, from which mAb-AEVB was selected, because hydrazone-linked drugs have played a prominent role in targeted drug therapy<sup>8-11,30</sup>. In addition, we investigated dipeptide linkers, on the basis of earlier reported stability characteristics of peptide conjugates of daunorubicin and doxorubicin<sup>16-20</sup>, drugs with much lower potencies than the auristatins. It is demonstrated here that the peptide linkers are efficiently hydrolyzed by cathepsin B and lead to conjugates that are highly immunospecific *in vitro*. In the first detailed comparison of the peptide versus hydrazone drug-linking strategies, we found that the peptide linkers were superior in almost all respects.

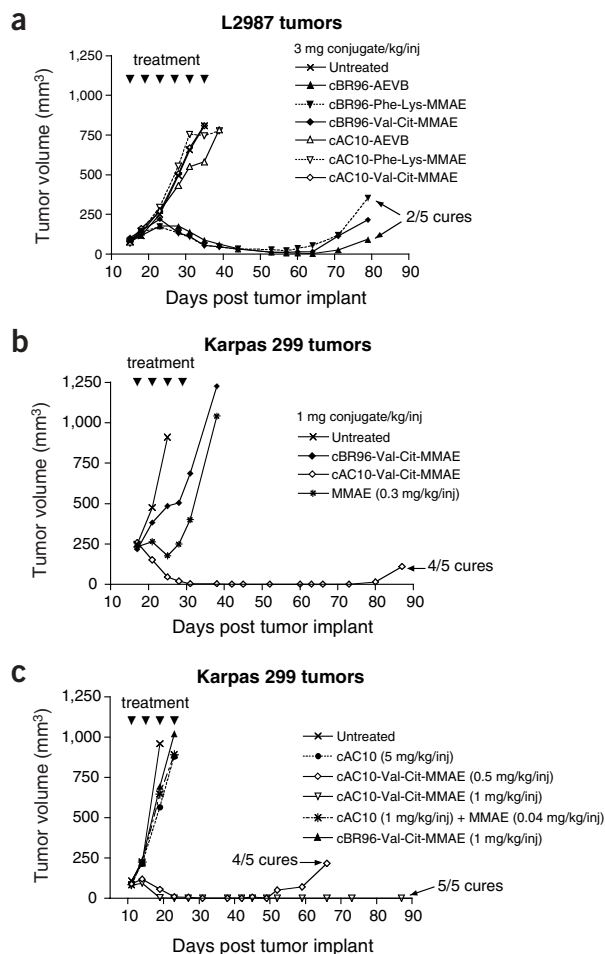
The conjugates with the most promising characteristics based on *in vitro* cytotoxicity and specificity, plasma stability, toxicity and *in vivo* therapy consisted of mAb-Val-Cit-MMAE with approximately eight drug units per mAb. Drug loading was established by spectral and thiol group analyses, amino acid analysis, matrix-assisted desorption ionization (MALDI) MS and quantitation of released drug after enzymatic hydrolysis. The results using a variety of IgGs,

including cBR96 and cAC10 as reported here, suggest that the chemistry is widely applicable and leads to a high degree of conjugate uniformity, in contrast with other methods using the random modification of mAb lysine residues<sup>11-14</sup>. This latter aspect is important for future drug development.

An indication of the scope of the conjugation technology described here is apparent from the activities obtained in widely dissimilar tumor models. cBR96-Val-Cit-MMAE and cAC10-Val-Cit-MMAE effected cures and regressions of established lung adenocarcinoma and ALCL tumors with complete immunological specificity at low and very well-tolerated conjugate doses. Similar results with these and other mAb-Val-Cit-MMAE have been obtained in breast and ovarian carcinoma, and in hematological diseases such as multiple myeloma and Hodgkin's disease (data not shown).

The therapeutic window of cAC10-Val-Cit-MMAE in the ALCL model is significantly improved over other mAb-drug conjugate designs. CD30 may be an appropriate target antigen to test the first mAb-Val-Cit-MMAE conjugate in the clinic, because it has very restricted expression in normal tissues but is widely expressed in Hodgkin's disease, ALCL, non-Hodgkin's lymphoma, multiple

**Figure 5** *In vivo* therapeutic efficacy of the conjugates in immunocompromised mice with subcutaneous human tumor xenografts. (a) Athymic mice with subcutaneous L2987 human lung adenocarcinoma tumors (cBR96 Ag<sup>+</sup>, cAC10 Ag<sup>+</sup>) were treated with the conjugates (3 mg mAb component/kg/injection, administered i.v.) according to the treatment schedule indicated by the arrowheads. (b) SCID mice with subcutaneous Karpas 299 human ALCL tumors (cAC10 Ag<sup>+</sup>, cBR96 Ag<sup>+</sup>) were treated with MMAE (0.3 mg/kg/injection) or with the mAb-Val-Cit-MMAE (1 mg mAb component/kg/injection corresponding to 0.03 mg drug component/kg/injection; 1/30th of the conjugate MTD) according to the treatment schedule shown. (c) SCID mice with Karpas 299 tumors were treated with cAC10, cAC10 + unconjugated MMAE, cAC10-Val-Cit-MMAE or cBR96-Val-Cit-MMAE at the doses indicated. The experiments incorporated five mice per group and were reproducible in at least three independent studies.



© 2003 Nature Publishing Group http://www.nature.com/naturebiotechnology



myeloma and cutaneous T-cell lymphoma<sup>28</sup>. It is probable that not only would such malignancies be more accessible to the macromolecular drug than solid tumors, but they would also be expected to be more chemosensitive. These issues, together with the intrinsic properties of cAC10-Val-Cit-MMAE, may have contributed to the ability to use doses as low as 1/60th of the MTD and still achieve therapeutic efficacy in a CD30<sup>+</sup> ALCL tumor model. We are currently evaluating the effects of cAC10-Val-Cit-MMAE in other CD30<sup>+</sup> tumors, some of which are multidrug resistant, and establishing its toxicity and pharmacokinetic profiles, as we move toward the development of this promising conjugate for clinical trials.

## METHODS

The IgG<sub>1</sub> chimeric mAbs cAC10 (ref. 28) and cBR96 (ref. 10) recognize the CD30 and Lewis Y antigens, respectively. H3396 human breast carcinoma<sup>31</sup>, RCA human colorectal carcinoma<sup>10</sup>, and L2987 human lung adenocarcinoma<sup>10</sup> cell lines have been described elsewhere. Karpas 299 ALCL cells were obtained from the Deutsche Sammlung von Mikroorganismen und Zellkulturen GMBH (Braunschweig, Germany). AE was prepared according to a published method<sup>25</sup>. MMAE was similarly prepared, substituting Fmoc-protected *N*-methylvaline for *N,N*-dimethylvaline in the synthesis. After chromatography, pure MMAE (by HPLC, MS, <sup>1</sup>H-NMR and <sup>13</sup>C-NMR, and elemental analysis) was obtained as a white powder.

**Maleimidocaproyl-peptide-MMAE derivatives.** Maleimidocaproyl-Val-Cit-*p*-aminobenzyl alcohol *p*-nitrophenylcarbonate<sup>16</sup> (2.6 g, 3.52 mmol, 1.5 equiv.), MMAE (1.69 g, 2.35 mmol, 1 equiv.) and *N*-hydroxybenzotriazole (64 mg, 0.45 mmol, 0.2 equiv.) were stirred in 25 ml dimethyl formamide for 2 min. Pyridine (5 mM) was added, and after 24 h the solvent was removed. The product was purified using C<sub>18</sub> reversed-phase preparative HPLC (RP-HPLC), providing 1.78 g (57%) of amorphous white powder that was >95% pure by HPLC. The <sup>1</sup>H-NMR was consistent with the proposed structure. Electrospray (ES)-MS *m/z* 1316.7 [M + H]<sup>+</sup>; UV λ<sub>max</sub> 215, 248 nm. Maleimidocaproyl-Phe-Lys-*p*-aminobenzyl alcohol *p*-nitrophenylcarbonate<sup>16</sup> was similarly coupled to MMAE to prepare maleimidocaproyl-Phe-Lys-MMAE. The product was >95% pure by HPLC and the <sup>1</sup>H-NMR was consistent with the structure. MS *m/z* 1334.8 [M + H]<sup>+</sup>; UV λ<sub>max</sub> 215, 256 nm.

**Maleimidocaproyl-AEVB.** 5-Benzoylvaleric acid (30 mg, 0.14 mmol, 2 equiv.) was added to a solution of AE (50 mg, 0.07 mmol, 1 equiv.) in anhydrous CH<sub>2</sub>Cl<sub>2</sub> (2 ml), followed by *N,N'*-dicyclohexylcarbodiimide (30 mg, 0.14 mmol, 2 equiv.) and 4-dimethylaminopyridine (5 mg). The mixture was stirred overnight at 23 °C, filtered, and the product purified after workup by preparative chromatography on silica gel using a step gradient of MeOH in CH<sub>2</sub>Cl<sub>2</sub>. The yield was 50 mg (78%) of white solid; UV λ<sub>max</sub> 215 nm. High resolution MS found *m/z* 920.6139 [M + H]<sup>+</sup>; calculated for C<sub>52</sub>H<sub>82</sub>N<sub>5</sub>O<sub>9</sub> 920.6113. The <sup>1</sup>H-NMR was consistent with the structure.

6-Maleimidocaproylhydrazide (190 mg, 0.51 mmol, 4.7 equiv.; Molecular Biosciences Inc.) was added to a solution of AEVB (100 mg, 0.11 mmol) in 0.01% trifluoroacetic acid (TFA) in MeOH (2 ml). The mixture was stirred at 23 °C for 12 h. The product was isolated by C<sub>18</sub> RP-HPLC, yielding maleimidocaproyl-AEVB as a white solid (97 mg, 78%); UV λ<sub>max</sub> 215, 280 nm. HR-MS found *m/z* 1127.7132 [M + H]<sup>+</sup>; calculated for C<sub>62</sub>H<sub>95</sub>N<sub>8</sub>O<sub>11</sub> 1127.7120. The <sup>1</sup>H-NMR was consistent with the structure.

**Conjugate preparation.** The mAbs (>5 mg/ml) in PBS containing 50 mM borate, pH 8.0, were treated with dithiothreitol (10 mM final) at 37 °C for 30 min. After gel filtration (G-25, PBS containing 1 mM DTPA), thiol determination using 5,5'-dithiobis(2-nitrobenzoic acid) indicated that there were approximately eight SH groups per mAb. To the reduced mAbs at 4 °C was added the maleimido drug derivatives (1.1 equiv./SH group) in cold CH<sub>3</sub>CN (20% v/v). After 1 h, the reactions were quenched with excess cysteine, the conjugates were concentrated by centrifugal ultrafiltration, gel filtered (G-25, PBS) and sterile filtered. Protein and drug concentrations were determined by spectral analysis, residual thiol group assays and amino acid analysis. Size-exclusion HPLC established that all conjugates used in this study were >98% monomeric,

and C<sub>18</sub> RP-HPLC established that there was <0.5% unconjugated cysteine-quenched drug. Yields were in the range of 80% based on the mAb component. The uniformity of the conjugates obtained was consistent with earlier reports for cBR96-doxorubicin<sup>10</sup>.

**Binding studies.** RCA cells (3 × 10<sup>6</sup> cells/ml, 100 l) were treated with serial dilutions of cBR96 and cBR96 conjugates in PBS. After 30 min at 4 °C, the cells were washed and resuspended in PBS at 4 °C. Secondary goat antibody specific to human F(ab)<sub>2</sub>-fluorescein isothiocyanate (Jackson ImmunoResearch) was added to the cells and incubation was continued for 30 min on ice. The cells were washed, fixed with 1% paraformaldehyde and analyzed by flow cytometry.

**Plasma stability.** The conjugates (0.33 mg/ml) were incubated in triplicate in normal human or mouse plasma at 37 °C. At periodic intervals, aliquots (50 l) were removed and spiked with a related auristatin analog as an internal standard. For the MMAE conjugates, H<sub>3</sub>PO<sub>4</sub> (10 l, 2.9 M) was added, and the samples were subjected to solid-phase extraction (Oasis MCX cartridges; Waters Corp.). The cartridges were washed with 0.1 M HCl and then CH<sub>3</sub>OH, and the free drug was eluted with 5% NH<sub>4</sub>OH in CH<sub>3</sub>OH. Solvents were removed under reduced pressure, and the samples were reconstituted and analyzed by LC-MS/MS using a C<sub>18</sub> reversed-phase column. For the AEVB conjugates, instead of extracting from solid phase the drug was separated from plasma proteins by adding one volume of cold CH<sub>3</sub>CN and then centrifuging at 15,700g for 5 min.

**Cytotoxicity assays.** Karpas 299, H3396 and RCA cells in RPMI-1640 medium containing 10% FBS were plated at 10,000, 5,000 and 5,000 cells/well, respectively. The cells were treated with conjugates or free drug for the times indicated in the figures. For pulsed drug treatments, the cells were washed and incubation was continued up to the 92 h post-drug treatment time point. Alamar Blue (Biosource International; diluted 2.5-fold with medium) was added so that the final amount was 10% of the culture volume. The cells were incubated an additional 4 h, and dye reduction was measured on a fluorescent plate reader.

For the clonogenic assay, adherent RCA cells (overnight culture of 10<sup>5</sup> cells/well in six-well dishes containing 5 ml of medium) were treated with fresh medium containing dilutions of cBR96-Val-Cit-MMAE or control nonbinding conjugate, and the cultures were incubated at 37 °C for 96 h. Cells were then trypsinized and counted. Replicate plates were plated at 100, 1,000 and 10,000 cells/plate in 5 ml of medium, and incubation was continued for 10 d at 37 °C. After removing the medium, the cultures were washed with PBS and 0.25% Coomassie Blue was added. Colonies of ≥50 cells were counted.

**In vivo experiments.** All procedures were approved by the Animal Care and Use Committee (NIH animal welfare assurance no. A4247-01). Karpas 299 cells (5 × 10<sup>6</sup>) were implanted in the right flank of CB17 SCID mice, and were allowed to grow to the sizes indicated in the figures, at which time therapy was initiated by injecting solutions of the conjugates or MMAE in PBS intravenously (tail vein) at the doses indicated in the text. Similar methods were used for L2987 solid tumors<sup>10</sup>, which were implanted into BALB/c athymic mice after *in vivo* passaging.

## ACKNOWLEDGMENTS

This work was supported in part by Grant 1R43 CA 88583-01A1 from the National Cancer Institute. We acknowledge George Robert Pettit, Nathan Ihle and Perry Fell for useful discussions, and Nick Vincent-Maloney, Starr Rejniak and Jennifer Haugen for experimental assistance.

## COMPETING INTERESTS STATEMENT

The authors declare that they have no competing financial interests.

Received 6 January; accepted 25 March 2003

Published online 1 June 2003; doi:10.1038/nbt832

1. Carter, P. Improving the efficacy of antibody-based cancer therapies. *Nat. Rev. Cancer* **1**, 118–129 (2001).
2. Dillman, R.O. Monoclonal antibodies in the treatment of malignancy: basic concepts and recent developments. *Cancer Invest.* **19**, 833–841 (2001).
3. King, K.M. & Younes, A. Rituximab: review and clinical applications focusing on non-Hodgkin's lymphoma. *Expert Rev. Anticancer Ther.* **1**, 177–186 (2001).
4. Schwartzberg, L.S. Clinical experience with edrecolomab: a monoclonal antibody therapy for colorectal carcinoma. *Crit. Rev. Oncol. Hematol.* **40**, 17–24 (2001).

5. Yarden, Y. & Sliwkowski, M.X. Untangling the ErbB signaling network. *Nat. Rev. Mol. Biol.* **2**, 127–137 (2001).
6. Dubowchik, G.M. & Walker, M.A. Receptor-mediated and enzyme-dependent targeting of cytotoxic anticancer drugs. *Pharmacol. Ther.* **83**, 67–123 (1999).
7. Bross, P.F. *et al.* Approval summary: gemtuzamab ozogamicin in relapsed acute myeloid leukemia. *Clin. Cancer Res.* **7**, 1490–1496 (2001).
8. Hamann, P.R. *et al.* An anti-CD33 antibody calicheamicin conjugate for treatment of acute myeloid leukemia. Choice of linker. *Bioconjug. Chem.* **13**, 40–46 (2002).
9. Hamann, P.R. *et al.* Gemtuzamab ozogamicin, a potent and selective anti-CD33 antibody-calicheamicin conjugate for treatment of acute myeloid leukemia. *Bioconjug. Chem.* **13**, 47–58 (2002).
10. Trail, P.A. *et al.* Cure of xenografted human carcinomas by BR96-doxorubicin immunoconjugates. *Science* **261**, 212–215 (1993).
11. Saleh, M.N. *et al.* Phase I trial of anti-Lewis Y drug immunoconjugate BR96-doxorubicin in patients with Lewis Y-expressing epithelial tumors. *J. Clin. Oncol.* **18**, 2282–2292 (2000).
12. Liu, C. *et al.* Eradication of large colon tumor xenografts by targeted delivery of maytansinoids. *Proc. Natl. Acad. Sci. USA* **93**, 8618–8623 (1996).
13. Chari, R.V.J. *et al.* Enhancement of the selectivity and antitumor efficacy of a CC-1065 analogue through immunoconjugate formation. *Cancer Res.* **55**, 4079–4084 (1995).
14. Ojima, I. *et al.* Tumor-specific novel taxoid monoclonal antibody conjugates. *J. Med. Chem.* **45**, 5620–5623 (2002).
15. Jain, R.K. Physiological barriers to delivery of monoclonal antibodies and other macromolecules in tumors. *Cancer Res.* **50**, 814–819 (1990).
16. Dubowchik, G.M. *et al.* Cathepsin B-labile dipeptide linkers for lysosomal release of doxorubicin from internalizing immunoconjugates: model studies of enzymatic drug release and antigen-specific *in vitro* anticancer activity. *Bioconjug. Chem.* **13**, 855–869 (2002).
17. King, H.D. *et al.* Monoclonal antibody conjugates of doxorubicin prepared with branched peptide linkers: inhibition of aggregation by methoxytriethyleneglycol chains. *J. Med. Chem.* **45**, 4336–4343 (2002).
18. Toki, B.E., Cerveny, C.G., Wahl, A.F. & Senter, P.D. Protease-mediated fragmentation of *p*-amidobenzyl ethers: a new strategy for the activation of anticancer prodrugs. *J. Org. Chem.* **67**, 1866–1872 (2002).
19. de Groot, F.M., Damen, E.W. & Scheeren, H.W. Anticancer prodrugs for application in monotherapy: targeting hypoxia, tumor associated enzymes, and receptors. *Curr. Med. Chem.* **8**, 1093–1122 (2001).
20. Trouet, A., Masquelier, M., Baurain, R. & Deprez-De Campeneere, D. A covalent linkage between daunorubicin and proteins that is stable in serum and reversible by lysosomal hydrolases, as required for a lysosomotropic drug-carrier conjugate: *in vitro* and *in vivo* studies. *Proc. Natl. Acad. Sci. USA* **79**, 626–629 (1982).
21. Pettit, G.R. The dolastatins. *Fortschr. Chem. Org. Naturst.* **70**, 1–79 (1997).
22. Vaishampayan, U. *et al.* Phase II study of dolastatin-10 in patients with hormone-refractory metastatic prostate adenocarcinoma. *Clin. Cancer Res.* **6**, 4205–4208 (2000).
23. Madden, T. *et al.* Novel marine-derived anticancer agents: a phase I clinical, pharmacological, and pharmacodynamic study of dolastatin 10 (NSC 376128) in patients with advanced solid tumors. *Clin. Cancer Res.* **6**, 1293–1301 (2000).
24. Otani, M. *et al.* TZT-1027, an antimicrotubule agent, attacks tumor vasculature and induces tumor cell death. *Jpn. J. Cancer Res.* **91**, 837–844 (2000).
25. Pettit, G.R. & Barkoczy, J. Tumor inhibiting tetrapeptide bearing modified phenethyl amides. US 5,635,483 (1997).
26. Carl, P.L., Chakravarty, P.K. & Katzenellenbogen, J.A. A novel connector linkage applicable in prodrug design. *J. Med. Chem.* **24**, 479–480 (1982).
27. Koblinski, J.E., Ahram, M. & Sloane, B.F. Unraveling the role of proteases in cancer. *Clin. Chim. Acta* **291**, 113–135 (2000).
28. Wahl, A.F. *et al.* The anti-CD30 monoclonal antibody SGN-30 promotes growth arrest and DNA fragmentation *in vitro* and affects antitumor activity in models of Hodgkin's disease. *Cancer Res.* **62**, 3736–3742 (2002).
29. Satoh, T. & Hosokawa, M. The mammalian carboxylesterases: from molecules to functions. *Annu. Rev. Pharmacol. Toxicol.* **38**, 257–288 (1998).
30. Schrappe, M. *et al.* Long-term growth suppression of human glioma xenografts by chemoimmunoconjugates of 4-desacetylvinblastine-3-carboxyhydrazide and monoclonal antibody 9.2.27. *Cancer Res.* **52**, 3838–3844 (1992).
31. Wallace, P.M. & Senter, P.D. *In vitro* and *in vivo* activities of monoclonal antibody-alkaline phosphatase conjugates in combination with phenol mustard phosphate. *Bioconjug. Chem.* **2**, 349–352 (1991).

---

## Erratum: Development of potent monoclonal antibody auristatin conjugates for cancer therapy

Svetlana O Doronina, Brian E Toki, Michael Y Torgov, Brian A Mendelsohn, Charles G Cerveny, Dana F Chace, Ron L DeBlanc, R Patrick Gearing, Tim D Bovee, Clay B Siegall, Joseph A Francisco, Alan F Wahl, Damon L Meyer & Peter D Senter  
*Nat. Biotechnol.* 21, 778–784 (2003)

In the legend to **Figure 4d** on page 781, cIgG Ag<sup>-</sup> should be cAC10 Ag<sup>-</sup>.

---

## Corrigendum: A model of molecular interactions on short oligonucleotide microarrays

Li Zhang, Michael F Miles & Kenneth D Aldape  
*Nat. Biotechnol.* 21, 818–821 (2003)

In the legend to **Figure 1** on page 819, text in parts **b** and **c** was transposed. The legend should have read as follows:

(**b**) Weight factors. (**c**) Nearest-neighbor stacking energy. These stacking energies weakly correlated ( $r = 0.6$ ) with that found in aqueous solution<sup>8</sup>, and are smaller in magnitude.

In the legend to **Figure 2** on page 820, figure parts were referred to incorrectly. The legend should have read as follows:

Accuracy test. Known concentrations of 14 'spike-in' genes are compared with those obtained from (a) PDNN, (b) MAS5.0 and (c) dChip. Each line represents a gene in 14 samples. The microarray raw data were obtained from the '1532 series' human data (see Methods for URL). For genes other than the 'spike-ins', standard deviations (s.d.) versus the averages of the log-transformed expression levels are shown in **d**, **e** and **f** as determined using PDNN, MAS5.0 and dChip<sup>7</sup>, respectively. Each of these figures contains 12,474 genes; top half shown in red.